

Accepted Manuscript

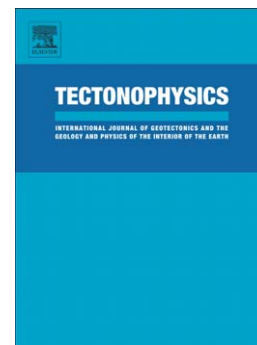
Ambient noise tomography reveals basalt and sub-basalt velocity structure beneath the Faroe Islands, North Atlantic

Carmelo Sammarco, David G. Cornwell, Nicholas Rawlinson

PII: S0040-1951(17)30380-3
DOI: doi:[10.1016/j.tecto.2017.09.012](https://doi.org/10.1016/j.tecto.2017.09.012)
Reference: TECTO 127625

To appear in: *Tectonophysics*

Received date: 21 March 2017
Revised date: 12 September 2017
Accepted date: 14 September 2017



Please cite this article as: Sammarco, Carmelo, Cornwell, David G., Rawlinson, Nicholas, Ambient noise tomography reveals basalt and sub-basalt velocity structure beneath the Faroe Islands, North Atlantic, *Tectonophysics* (2017), doi:[10.1016/j.tecto.2017.09.012](https://doi.org/10.1016/j.tecto.2017.09.012)

This is a PDF file of an unedited manuscript that has been accepted for publication. As a service to our customers we are providing this early version of the manuscript. The manuscript will undergo copyediting, typesetting, and review of the resulting proof before it is published in its final form. Please note that during the production process errors may be discovered which could affect the content, and all legal disclaimers that apply to the journal pertain.

Ambient noise tomography reveals basalt and sub-basalt velocity structure beneath the Faroe Islands, North Atlantic

Carmelo Sammarco^a, David G. Cornwell^a, Nicholas Rawlinson^{a,b}

^a*School of Geosciences, University of Aberdeen, King's College, Aberdeen, AB24 3UE, UK.*

^b*Bullard Laboratories, Department of Earth Sciences, University of Cambridge, Madingley Road, Cambridge, CB3 0EZ, UK.*

Abstract

Ambient noise tomography is applied to seismic data recorded by a portable array of seismographs deployed throughout the Faroe Islands in an effort to illuminate basalt sequences of the North Atlantic Igneous Province, as well as underlying sedimentary layers and Precambrian basement. Rayleigh wave empirical Green's functions between all station pairs are extracted from the data via cross-correlation of long-term recordings, with phase weighted stacking implemented to boost signal-to-noise ratio. Dispersion analysis is applied to extract inter-station group travel-times in the period range 0.5–15 s, followed by inversion for period-dependent group velocity maps. Subsequent inversion for 3-D shear wave velocity reveals the presence of significant lateral heterogeneity (up to 25%) in the crust. Main features of the final model include: (i) a near-surface low velocity layer, interpreted to be the Malinstindur Formation, which comprises subaerial compound lava flows with a weathered upper surface; (ii) a sharp velocity increase at the base of the Malinstindur Formation, which may mark a transition to the underlying Beinivörð For-

mation, a thick laterally extensive layer of subaerial basalt sheet lobes; (iii) a low velocity layer at 2.5–7.0 km depth beneath the Beinisdvørð Formation, which is consistent with hyaloclastites of the Lopra Formation; (iv) an upper basement layer between depths of 5–9 km and characterized by S wave velocities of approximately 3.2 km/s, consistent with low-grade metamorphosed sedimentary rocks; (v) a high velocity basement, with S wave velocities in excess of 3.6 km/s. This likely reflects the presence of a crystalline mid-lower crust of Archaean continental origin. Compared to previous interpretations of the geological structure beneath the Faroe Islands, our new results point to a more structurally complex and laterally heterogeneous crust, and provide constraints which may help to understand how continental fragments are rifted from the margins of newly forming ocean basins.

Keywords: Seismic tomography, ambient seismic noise, North Atlantic, crustal structure

1. Introduction

The crustal structure of the continental block on which the Faroe Islands (Fig. 1) sits is poorly understood, largely due to the presence of thick Tertiary basalt sequences of the North Atlantic Igneous Province at the surface that hinder controlled-source seismic imaging methods (e.g. Maresh et al., 2006). The region is of particular interest for: i) examining magma-assisted break-up of continents (e.g. Kendall et al., 2005), due to its proximity to the ocean-continent boundary; and ii) locating offshore hydrocarbon prospects within the Faroese sector of the Faroe Shetland Basin, since they are expected to occur both in layered basalt flows (including hyaloclastites) and in

sediments between the base of basaltic sequences and the top of Precambrian crystalline basement. The onshore thickness of the basalts, the presence of sub-basalt sediments and the depth and lateral variation of the underlying crystalline basement, however, are largely unconstrained. In this study, we use data from a 12-station temporary seismic array and apply the passive seismological method of ambient noise tomography to construct a 3-D shear wave velocity model for the uppermost ~ 15 km beneath the Faroe Islands. Through interpretation of lateral and depth variations in velocity structure, we are able to delineate for the first time the extent and internal properties of the basalt pile, together with the structural configuration of the underlying layers.

1.1. Geology of the Faroe Islands

The Faroe Islands Basalt Group (FIBG) (Fig. 1) was emplaced during Paleocene and Eocene times and formed part of the North Atlantic Igneous Province (NAIP) magmatism (Upton, 1988; Waagstein, 1988; Saunders et al., 1997; Meyer et al., 2007), which was emplaced via subaerial volcanism during the separation of Greenland and Eurasia. The FIBG areal extent is at least $120,000 \text{ km}^2$ within the NE Atlantic region and it is exposed throughout the $\sim 1400 \text{ km}^2$ surface area of the 18 main islands that comprise the Faroe Islands (Passey and Jolley, 2008) (Fig. 2). Post-emplacment subsidence is a likely explanation for the origin of the present-day FIBG dip of $<4^\circ$ in an E-SE direction (Andersen, 1988) and its stratigraphic thickness totals at least $\sim 6.6 \text{ km}$ (Rasmussen and Noe-Nygaard, 1969, 1970; Waagstein, 1988; Passey and Bell, 2007; Passey and Jolley, 2008).

The FIBG consists of basalt lava flows with minor volcanoclastic (sedi-

mentary and pyroclastic) lithologies, and the major formations from base to top are: 1) Lopra Formation: at least ~ 1.1 km thick and composed of volcanoclastic lithologies, mainly hyaloclastites (Ellis et al., 2002; Waagstein and Andersen, 2003; Passey and Jolley, 2008); 2) Beinisvørð Formation: ~ 3.25 km thick laterally extensive, subaerial basalt sheet lobes topped by an erosional surface (Passey and Bell, 2007); 3) Malinstindur Formation: < 1.4 km thick subaerial compound lava flows with a weathered upper surface (Passey and Bell, 2007); 4) Enni Formation: > 900 m thick subaerial compound lava flows and sheet lobes (Passey and Jolley, 2008). Sub-vertical dykes have intruded most levels of the basalt, along with irregular and saucer-shaped sills (Hansen et al., 2011). Erosion may have removed at least a few hundred metres of the Enni Formation, assuming it was uniformly distributed with an original thickness of 1.0–1.5 km (Waagstein, 1988; Andersen et al., 2002).

The FIBG rocks exposed on the Faroe Islands are presumed to either rest atop pre-Cretaceous (Brewer and Smythe, 1984) sedimentary rocks or Lewisian crystalline basement. Seismic refraction experiments revealed offshore sedimentary sequences that reach thicknesses of: i) a few kilometres but appear to pinch out towards the Faroe Islands (Richardson et al., 1999); ii) 7–8 km offshore and 3–4 km beneath the Faroe Islands (Raum et al., 2005); or iii) less than 1 km beneath central regions and up to 3 km beneath northern and southern parts of the Faroe Islands (White et al., 2003). Ambiguity remains due to multiple ways of interpreting a sub-basalt layer with a P -wave velocity of 5.2–5.7 km/s and the possible contamination of sub-basalt sedimentary rocks with igneous sill intrusions (Richardson et al., 1999; England et al., 2005; Raum et al., 2005). Lewisian basement rocks are

exposed in East Greenland and Shetland Islands (Stoker et al., 1993) and it is therefore expected that Archaean to Proterozoic age Lewisian metamorphic rocks comprise the crystalline basement beneath the Faroe Islands. This is most likely underlain by stretched Archaean continental crust that could be thickened and/or intruded by magmatic material (Bott et al., 1974; Richardson et al., 1998; Raum et al., 2005).

1.2. Previous Geophysical and Borehole Studies

Regional refraction and wide-angle reflection profiles have been acquired to investigate the crustal structure to the northeast, east and southeast of the Faroe Islands (Fig. 1). It is widely agreed that the velocity structure most likely represents crystalline crust with a continental composition (Bott et al., 1974; Richardson et al., 1998, 1999; Smallwood et al., 1999; Raum et al., 2005). Moho depths along these profiles vary between 17 and 35 km, while estimates of crustal thickness beneath the Faroe Islands are either 21–32 km (through extrapolation onshore from the seismic profiles) or 27–38 km (described as ~ 30 km) from an onshore seismic refraction study (Bott et al., 1974).

A map of basalt and sub-basalt sedimentary layer thickness beneath the Faroe Islands and surrounding area, compiled from published wide-angle seismic data, indicates that basalt thickness is consistently 5.5–6.0 km across the majority of the Faroe Islands apart from 4.5–5.5 km and 3.5–4.5 km beneath the southern islands of Sandoy and Suðuroy, respectively (White et al., 2003). Sub-basalt sediment thickness was estimated to be ≤ 1.5 km beneath the central Faroe Islands, increasing to 2–3 km in northeastern and southern parts. A more recent seismic profile showed evidence for a 2–3 km thick low velocity

sub-basalt Mesozoic sedimentary layer (Raum et al., 2005). The geophysical properties of key layers included in published models of Faroe Islands crustal structure are shown in Table 2 (Palmason, 1965; Richardson et al., 1999; Smallwood et al., 1999; England et al., 2005; Raum et al., 2005; Christie et al., 2006; Eccles et al., 2007; Bais et al., 2008; Petersen et al., 2013). The main information for the Glyvursnes-1, Vestmanna-1 and Lopra-1A boreholes are summarised in Table 3 (from Waagstein and Andersen, 2003; Petersen et al., 2013, and references therein). In addition to Table 3 Lopra-1 was drilled to a depth of 2178 m in 1981 and subsequently deepened to 3565 m in 1996. The original Lopra-1 borehole penetrated through ~ 2 km of the Beinivørð Formation and the deepened Lopra-1A section additionally penetrated 213 m of the Beinivørð Formation, then 45 m of pillow lavas, followed by 41 m of pillow lava debris atop a thick series of volcanic tuffs (including intra-volcanic sand-stone and clay-stone) of the uppermost Lopra Formation. The base of the volcanic rocks was not encountered (Heinesen et al., 2006). The Beinivørð Formation is characterized by high frequency variations in P -wave velocity between 4 and 6 km/s (similar to the Enni Formation) whereas the Lopra Formation shows S -wave velocities of 2.5–3.5 km/s where $V_S \approx 2.6$ km/s for hyaloclastite and $V_S \approx 2.8$ km/s for hyaloclastite interspersed with basalt beds. V_P/V_S is 1.81–1.84 (Christie et al., 2006; Petersen et al., 2013).

2. Data and Method

2.1. Faroe Islands Passive Seismic Experiment (FIPSE)

The data for this study was recorded by the Faroe Islands Passive Seismic Experiment (FIPSE), which comprised 12 broadband seismic stations (Fig. 2)

that spanned the Faroe Islands. The array operated for 17 months between June 2011 and October 2012 with an average data return of $\sim 86\%$ with equipment failures due to the effects of high winds and heavy rain on stations IF06 (74%), IF11 (62%) and IF12 (37%). Each station was equipped with a Gralp CMG-3ESPD (60 sec to 50 Hz) seismometer recording continuous 3-component data at 100 samples per second (sps), deployed directly onto the basalt bedrock and buried under 1.0-1.5 m of topsoil.

2.2. Cross-correlation to extract Empirical Green's functions

Our process to extract Empirical Green's functions (EGF) through cross-correlation of ambient noise is similar to that described by Bensen et al. (2007). Hour-long segments of the vertical component of ground motion for each of the FIPSE stations (Fig. 2) were downsampled to 1 sps, had their instrument response, mean and trend removed and were band-passed between 0.05 and 2.0 Hz. Earthquake signals and local noise spikes that may contaminate the ambient noise wave-field were diminished by applying temporal normalization and spectral whitening. All simultaneously-recording station pairs were then cross-correlated using MSNoise (Lecocq et al., 2014) and its built-in ObsPy functions (Beyreuther et al., 2010; Megies et al., 2011) and then stacked into daily and full-recording period stacks using a phase weighted stacking (PWS) technique (Schimmel and Paulssen, 1997; Schimmel, 1999; Schimmel and Gallart, 2007). PWS enables detection of weak but coherent arrivals through exploiting the phase coherence in individual causal and a-causal correlograms and thereby improves the signal to noise ratio (SNR) in the stacks (Fig. 3). PWS has been widely used for enhancing cross-correlated signal extracted from ambient noise recordings (e.g. Ren et

al., 2013, Pilia, 2016), although some care in both its implementation and use is required to avoid distortion of the phase and amplitude characteristics of the waveform. In Figure S2 of the supplementary information, we compare the results of linear and phase weighted stacking and demonstrate that the the two methods produce similar results when the SNR is good, but that the PWS produces more realistic results when the SNR is poor.

2.3. Rayleigh wave group velocity dispersion analysis

Group velocity dispersion measurements were made by inputting the average of causal and a-causal (i.e. ‘symmetric’) cross correlation components from the 66 station pairs into a frequency-time analysis (FTAN) scheme (Dziewonski et al., 1969; Levshin et al., 1972). The symmetric component, in this case, is interpreted as the Rayleigh wave EGF (e.g. Curtis et al., 2006) and the automated pick of the peak amplitudes of the dispersion curves by FTAN provides a set of inter-station group travel-times across a range of periods (see Fig. 4 for an example. Supplementary Fig. S3 plots all the picked dispersion curves and their average). We cross-checked the results of FTAN with the Computer Programs in Seismology (CPS) code of Herrmann (2013) and found that they produced near identical results. Bensen et al. (2007) suggested that in order to measure group velocities reliably and accurately from cross-correlation functions (CCFs), the inter-station distance is required to be greater or equal to three wavelengths at a given period. Since this criterion limits the period to <10 s for the FIPSE array with its maximum aperture of ~ 100 km, we performed tests at different integer wavelength cutoffs and decided that an inter-station distance equal to two wavelengths was acceptable, thus permitting the use of group velocities up to a period

of ~ 15 s. As such, we tested three different cut-off wavelengths (1, 2 and 3) for group velocity measurements. In each case, we computed all dispersion curves and period dependent group velocity maps. For the 1 wavelength case, the standard deviation of all dispersion curves rapidly increased at longer periods (10-15 s), and the corresponding group velocity maps started to become incoherent and the data fit worse. For the 3 wavelength case, standard deviations remained relatively constant out to ~ 15 s period, but the decrease in available paths meant that resolution of the group velocity maps became poor at periods > 10 s. As such, we found that the 2 wavelength criterion gave the best compromise, in that it allowed longer period maps to be better constrained (up to 15 s), but produced results that were far more consistent with the 3 wavelength results compared to the 1 wavelength result (Supplementary Fig. S4). In a recent study, Luo et al. (2015) demonstrate that phase velocities can still be reliably measured at station separations as short as one wavelength, even when applying conventional time-domain cross-correlation to extract EGFs. In our case, a one-wavelength criterion does not produce good results, presumably due to the higher uncertainties associated with group velocity measurements compared to phase velocity measurements. Due to the small aperture of the seismic array, coupled with the apparent complexity of the crust beneath the Faroe Islands, we chose not to try and extract phase velocity because of the difficulty of overcoming the 2π phase ambiguity in the absence of long period data. To date, a number of studies (e.g. Pilia et al., 2015, Galetti et al., 2017, Green et al., 2017) have demonstrated that using approaches similar to ours, converting group velocity dispersion to 3-D shear wave-speed produces credible results which

can enhance our understanding of deep crustal structure.

One of the challenges of surface wave tomography is that it is difficult to estimate picking uncertainty from the dispersion analysis. With ambient noise data, one method for determining picking error is to compare dispersion curves constructed from different sub-sets of the data. Here, we subdivide the data into 30 day intervals and create dispersion curves for each interval. We set a minimum threshold of 45 cross-correlations (the maximum being 66) per time period, which resulted in seven different dispersion curves. For each station pair, we find the standard deviation of all available dispersion curves at each period, and then use this as an estimate of picking uncertainty, which is used to weight the travel-time data in the tomographic inversion for group velocity.

2.4. Period dependent group velocity maps

An iterative non-linear tomography scheme (Rawlinson et al., 2008) was employed to extract group velocity maps between 0.5 and 15.0 s period (Fig. 5). Smoothly varying cubic B-spline functions are used to describe the velocity continuum, which is controlled by a regular grid of nodes in latitude and longitude (grid intervals of 0.04° were used in this study). The forward problem of travel-time prediction is solved using the Fast Marching Method (Sethian, 1996; Rawlinson and Sambridge, 2004a,b) and a sub-space inversion technique (Kennett et al., 1988) is used to adjust model parameters to satisfy data observations. The two steps are applied iteratively to address the non-linear nature of the inverse problem. Strictly speaking, the geometric spreading of surface waves is a function of phase rather than group velocity; however, it is commonly assumed in ambient noise tomography (e.g.

Saygin and Kennett, 2012) that the phase and group velocity patterns will be similar at identical periods, in which case the path coverage determined using group velocities will be approximately correct. Damping and smoothing is used to regularize the inverse problem and produce a model that is as conservative as possible (i.e. not greatly perturbed from the initial model and with no unnecessary features) while still fitting the data to an acceptable level (e.g. Rawlinson and Sambridge, 2005). To find the best damping and smoothing parameters for the inversion, we plot the trade-off between model roughness/variance and data fit for different periods (Fig. 6). The point of maximum curvature should represent the optimum value of both parameters. In this way, we obtained optimum damping and smoothing factors of 0.005 and 0.007, respectively, by considering periods of 5, 10 and 15 s and used these damping and smoothing values for subsequent inversions.

A synthetic checkerboard test was performed to investigate the resolution of our group velocity maps between 0.5 s and 15 s period (Fig. 7). Three different synthetic models were generated that feature large (diameter ~ 18 km), medium (~ 12.5 km) and small (~ 7 km) anomalies with peak velocity perturbations of $\pm 20\%$; this provides insight into what wavelength of structure can be resolved in different parts of the model. The background or reference velocity is equal to the average velocity for each period (weighted by path length). The smallest checkerboard pattern is only recovered in the central northern part of the Faroe Islands below 5 s period (where path coverage is maximized). As the checkerboard size increases, both the region of good recovery increases and the period range over which recovery can be observed increases. Thus, we see that for the largest checkerboard anomalies, good

recovery throughout the Faroe Islands can be observed even at 10 s period. At 15 s period, the path coverage (Fig. 5) has reduced to such an extent that even the large checkerboard anomalies are poorly recovered. As a result, we limit our analysis of the subsequent shear wave velocity model, which is derived from the period dependent group velocity maps, to 10 km depth. Constraining shear wave-speeds below these depths requires group velocity measurements ≥ 15 s.

2.5. 3-D shear wave velocity model

In order to construct a 3-D shear wave velocity model of the crust from our group velocity maps, we first create an array of pseudo-dispersion curves by sampling the group velocity maps on a dense grid in latitude (grid spacing of 0.04°) and longitude (grid spacing of 0.05°). Inversion of each pseudo-dispersion curve produces a local 1-D shear wave velocity model, which can be combined with all other 1-D shear wave models to produce a composite 3-D shear wave velocity model. We use the CPS surface wave inversion codes (Herrmann, 2013) to recover 1-D shear wave velocity from group velocity dispersion. A damping value of 15 for the 1-D shear velocity model inversion was determined to be the best compromise from the data fit versus model variance trade-off curve (Fig. 8). In order to address the under-determined and non-linear nature of the inverse problem, we generate 100 starting models by applying Gaussian noise with a standard deviation of 0.3 km/s to our reference 1-D shear-wave velocity model, which is described in Table 1, and based on measurements from the three boreholes (see Fig. 1). Model parameters are defined at 0.5 km depth intervals in order to produce relatively smooth solution models. We perform an inversion for each starting model

at each point of the grid using 500 iterations of the scheme, and then take the average of the ensemble of solutions at each point as the final solution. The average standard deviation of the ensemble of solutions across the entire grid is 0.25 km/s, which is less than the standard deviation of the starting ensemble. The main features observed in horizontal (Fig. 9), south-north and west-east vertical (Fig. 10) slices through the final 3-D shear wave velocity model are described in the following section.

3. Results

3.1. Period dependent group velocity maps

The Rayleigh wave group velocity maps appear to reveal coherent velocity structure across periods from 0.5 to 12.0 s (Figure 5), with an increase in detail due to a higher concentration of stations in the north. Short period (0.5 and 1.0 s) maps reveal velocity variations over short (<20 km) length scales with a predominance of relatively fast velocity anomalies beneath the north-west and far south of the Faroe Islands. Longer period (5–12 s) group velocity maps, despite the presence of north-south smearing, show relatively low velocity anomalies beneath the north-west and central parts of the Faroe Islands, contrasting with fast anomalies in the north-east and south-west. While further interpretation may be possible, conversion of group velocity dispersion into a 3-D shear wave velocity model is more likely to yield a clearer picture of subsurface structure.

3.2. 3-D shear wave velocity model

At 1 km depth, the velocity pattern is quite variable across the model region, and may well contain artifacts due to noisy data and near surface

complexities that cannot be modeled (e.g. scattering caused by surface topography) using our approach. However, the lowest S wave velocities of <2.5 km/s occur beneath the north-west and central Faroe Islands. Relatively low (~ 2.6 km/s) velocities may also characterize the southernmost Faroese island of Suðuroy (Fig. 9). Between 3 and 5 km depth, the north-western region remains relatively slow (at 2.5–2.9 km/s) with a marked slow central anomaly (2.3–2.5 km/s). Surrounding central regions are typically constrained to 3.2–3.5 km/s and Suðuroy and south Sandoy ~ 2.8 km/s. Northeastern parts of the Faroe Islands appear to increase from 2.6–2.9 to 3.2–3.5 km/s between 3 and 5 km depth (Fig. 9).

Northeastern coastal regions are consistently fast at 3.5–3.7 km/s between 7 and 10 km depth, with north-central parts increasing from 3.0 to >3.5 km/s. Suðuroy displays S wave velocities of 3.2–3.5 km/s whereas the island of Sandoy to the north of Suðuroy is marked by relatively low (2.9–3.2 km/s) velocities (Fig. 9). The central region of the Faroe Islands at 15 km depth is characterized by a major low velocity anomaly where S wave velocities may be as low as 3.0 km/s and contrast markedly with the surrounding region at >3.5 km/s (Fig. 9).

The south-north and west-east cross-sections through the model in Figure 10 further highlight the large S wave velocity variations constrained beneath the Faroe Islands and surrounding coastal regions. A 1–2 km thick near-surface low (<2.5 km/s) velocity layer is most prominent in central and northern parts of the south-north profile and thickens from ~ 1 to ~ 3 km from west to east (Fig. 10), being thickest offshore. Beneath this, a higher S wave velocity (2.8–3.5 km/s) layer with a thickness of 2–4 km occurs in

the majority of the model, but appears absent (or unconstrained) in southern and western parts of the Faroe Islands. Examination of the upper and lower boundaries of this high velocity layer shows that it dips $\sim 4^\circ$ north and $1.5\text{--}2.5^\circ$ east. A deeper prominent low S wave velocity ($2.3\text{--}2.8$ km/s) layer can be identified in parts of the model where resolution allows. Its thickness varies between approximately 2 and 4 km and it is deepest in eastern and northern parts of the model (Fig. 10). However, it is unclear whether it extends beneath northernmost parts of the Faroe Islands' landmass. It sits atop a 2–3 km thick layer with S wave velocity ≈ 3.2 km/s and an abrupt increase in velocity with depth to ≥ 3.6 km/s. This rapid increase in velocity may reflect the presence of a seismic discontinuity between different rock types, which varies in depth between 6.5 km and 10.5 km where it is adequately sampled in the centre of the study region (Fig. 10). Lower S wave velocity ($3.0\text{--}3.3$ km/s) regions appear to intersperse with the higher velocity regions between 7.5 and 10.0 km in the model, although resolution is poorer at these depths.

4. Interpretation and Discussion

We now consider each of the basalt and sub-basalt layers that can be interpreted from major velocity variations in the model, from youngest to oldest.

4.1. Faroe Islands Basalt Group (FIGB): Enni and Malinstindur Formations

The near-surface (depth ≤ 1 km) low velocity regions described in the previous section coincide almost exactly with the surface outcrops of the Malinstindur Formation (Passey and Bell, 2007) (Fig. 1 and 9). Regions of elevated

S-wave velocity (2.8–3.4 km/s) at 1 km depth largely correspond to locations in the north-east and east of the Faroe Islands where the Enni Formation crops out at the surface (Passey and Bell, 2007) (Fig. 1). This is consistent with the typically higher *P* wave velocities for Enni compared with Malinstindur Formations from the Glyvursnes-1 borehole (Petersen et al., 2013) and references therein). Observations of higher *S* wave velocities in sheet flows (average $V_S=2.97$ km/s) compared with compound lava flows (average $V_S=2.52$ km/s) from the Lopra-1/1A borehole (Boldreel, 2006) are also in line with this velocity difference, since the Enni Formation contains a higher proportion of sheet lobes/flows than the compound flows of the Malinstindur Formation. Weathering of the uppermost layer of basalt is likely to account for the observed near-surface velocities of <2.5 km/s in the final model (e.g. Fig. 10).

The combined Enni and Malinstindur Formations may extend to 2 km depth in north-eastern parts of the Faroe Islands, evidenced by the observed low velocities in our model (Fig. 10a). However, in western parts of the Faroe Islands, the low velocity layer is considerably thinner and consistent with the 550–600 m thickness of Malinstindur Formation reported in the Vestmanna borehole (Waagstein and Hald, 1984) and from vertical seismic profile (VSP) experiments (Bais et al., 2008). Accordingly, we estimate the dip of the combined Enni and Malinstindur Formations (MF in Fig. 11) to be 1.5–2.5°NE from our *S* wave velocity model, which is similar to the onshore dip estimated using surface interpolation of 0–5°, with an average of 2°E–SE (Passey and Varming, 2010). Waagstein and Hald (1984) estimated an easterly dip of $\sim 4^\circ$ in the vicinity of the Vestmanna borehole (north-western

Faroe Islands, see Fig. 2).

4.2. Faroe Islands Basalt Group (FIGB): Beinivørð Formation

The ‘A’-horizon is a seismic discontinuity that marks the boundary between the Malinstindur and Beinivørð Formations that has been identified in onshore seismic, offshore seismic and VSP experiments. It is a prominent reflector that can be identified over much of the Faroese shelf, particularly when using seismic profiles reprocessed by TGS (OF94/95RE11), such as the Western Geophysical acquired OF94/95 which is located to the north-east of the Faroe Islands (Petersen et al., 2015). We show that this boundary also represents a major S wave velocity discontinuity between layers with $V_S < 2.5$ km/s above and $V_S = 2.8\text{--}3.5$ km/s below (Fig. 10) and interpret these layers to represent the Malinstindur and Beinivørð Formations, respectively.

The Vestmanna-1 and Lopra-1/1A boreholes sampled the uppermost ~ 100 m and the lowermost ~ 900 m of the Beinivørð Formation, respectively, and found typical average S wave velocities within the Beinivørð Formation of ~ 3.1 km/s for massive basalt flows and ~ 3.3 km/s for dolerite flows (Waagstein and Andersen, 2003). Variations in P wave velocity are 4–6 km/s and average $V_P/V_S = 1.84$ from both boreholes (Christie et al., 2006). These measurements are in agreement with our observations in Figures 9 and 10 and we constrain the locally fast Beinivørð Formation to dip $\sim 4^\circ$ north and $1.5\text{--}2.5^\circ$ east with a thickness of 2–4 km. Tracking similar relatively fast velocities indicates that the Beinivørð Formation may exist at depths of 3.5–5.5 km beneath northern Faroe Islands (Fig. 10). If this is the case, then the Beinivørð Formation may extend to depths previously interpreted as top basement (Palmason, 1965; Olavsdottir et al., 2016) (Fig. 11), but our

resolution in these regions appears to be unable to sufficiently distinguish the base Beinivørð / top basement interface beneath northern parts of our model (Fig. 10). Alternatively, there may be a reduction in S wave velocity difference across the ‘A’-horizon in these parts of the Faroe Islands.

We appear to lack the resolution to constrain a relatively fast velocity layer associated with the Beinivørð Formation beneath the southernmost (i.e. Suðuroy) and westernmost (i.e. Mykines) parts of the Faroe Islands (Figs. 2 and 10) but note that our modelled near surface (<2 km depth) S wave velocities are maximum in regions where the Beinivørð Formation crops out on the surface (Fig. 1 and 10).

4.3. Faroe Islands Basalt Group (FIGB): Lopra Formation and/or Sub-basalt Sediments

Offshore seismic profiles (Fig. 1) identify a low P wave velocity (3.8–4.1 km/s) layer that sits atop the basement beneath offshore parts of the profile (at 3–5 km depth on AMG95-1, 3–6 km on FLARE-1 and 4–7 km on FAST) but is interpreted to be absent below the Faroe Islands landmass (apart from AMG95-1) (Petersen and Funck, 2016, and references therein). We contend that this low velocity layer extends beneath the Faroe Islands landmass between depths of 2.5 and 7.0 km, is approximately 2–4 km thick and dips at $\sim 4^\circ$ to the north-east (Fig. 10 and 11).

The Lopra-1/1A borehole samples the uppermost ~ 1000 m of the Lopra Formation and is characterized by hyaloclastites which consist of lapilli-tuffs, tuff-breccias and breccias. Typical average S wave velocities within the Lopra Formation are markedly lower than for the Beinivørð Formation at ~ 2.6 km/s for intermingled layers of tuffs and brecciated hyaloclastites and

~ 2.8 km/s for tuffs/hyaloclastite interspersed with basalt flows (Waagstein and Andersen, 2003). These velocity ranges compare well with the observed $V_S=2.3\text{--}2.8$ km/s layer with a thickness of 2–4 km (Fig. 10) and therefore we are confident that this layer represents the Lopra Formation. Consistent with the overlying Beinisvørð Formation, it dips $\sim 4^\circ$ north and $1.5\text{--}2.5^\circ$ east.

Sub-basalt sediments reported from offshore seismic profiles that span the Faroe-Shetland Basin have a wide range of P wave velocities at 3.2–4.7 km/s (Petersen and Funck, 2016), and references therein), which translates into $V_S=1.9\text{--}2.8$ km/s assuming a V_P/V_S of 1.7 km/s. Unfortunately, this velocity range almost exactly matches that measured for the Lopra Formation and therefore it is difficult to assess the ratio of hyaloclastite to sediment within this low velocity layer using our method. However, we can show that a layer with the potential to include pre-volcanic sediments extends much further northwards beneath the Faroe Islands than previously thought and is consistent with the 2–3 km thick Mesozoic sedimentary layer identified by Raum et al. (2005).

4.4. Upper Basement

An ‘Upper Basement’ layer (between 5 and 7.5 km depth) is interpreted below the Lopra Formation / sub-basalt sediment layer with P wave velocities of ~ 5.75 km/s, V_P/V_S of 1.75 (and therefore $V_S \approx 3.3$ km/s) along some offshore profiles (Richardson et al., 1999). In particular, the basement velocity properties were noted to be distinctively lower beneath the Faroe island of Suðuroy than beneath the Faroe-Shetland Basin, with explanations ranging from pervasive weathering of existing Lewisian gneiss basement, modification by igneous processes or emplacement of tuffs at or near sea-level (Richardson

et al., 1999). This layer is consistent with a region in our model with $V_S \approx 3.2$ km/s that is distinct from the rapid increase in velocity beneath it that, in theory, should mark the top of the crystalline basement and therefore we interpret this intermediary region as a so-called upper basement layer. Its velocity properties are lower than typical continental upper crust and may be consistent with low-grade metamorphosed sedimentary rocks (e.g. Rudnick, 1995; Christensen and Mooney, 1995).

4.5. Crystalline Basement

Different offshore seismic velocity models map the crystalline basement between 5.0 and 7.5 km depth Petersen and Funck, 2016, with up to 1.5 km of topography on the basement discontinuity. These refraction and wide angle reflection profiles sample close to the southern Faroese Islands of Sandoy and Suðuroy and report P wave velocities of 6.1–6.3 km/s, V_P/V_S of 1.75 and therefore $V_S \approx 3.7$ km/s, which is consistent with our observations of a high-velocity ($V_S \geq 3.6$ km/s) basement-like feature at $\sim 61.75^\circ$ latitude (Fig. 10).

Despite diminishing resolution at basement depths at the extremities of our 3-D velocity model, we show that there may be major changes in basement topography beneath the Faroe Islands, possibly similar to those interpreted beneath the Norwegian margin (e.g. Osmundsen et al., 2002), which may correlate with the inferred positions of NW-trending faults or lineaments (Ritchie et al., 2011; Moy and Imber, 2009). Prolonged stretching of the Faroese crust, perhaps focussed in weaker parts of the crust, may have resulted in large offset faulting and the passage of magmatic material through the crust is likely to have altered and/or intruded the crystalline basement beneath the Faroe Islands.

5. Conclusions

Application of ambient noise tomography to a passive seismic dataset recorded by an array of broadband stations distributed throughout the Faroe Islands has allowed us to gain new insight into the upper-mid crustal structure of a poorly understood region of the North Atlantic margin. Key outcomes of this study include:

- A new 3-D shear wave velocity model of the crust beneath the Faroe Islands to a depth of ~ 10 km, with a maximum horizontal resolution of approximately 7 km in the upper crust beneath the northern region of the islands, where station density is greatest.
- A strong correlation between shear wave velocity variations with depth and the presence of volcanoclastic, sedimentary and crystalline rock layers that have previously been identified via drilling, nearby refraction profiling and surface mapping.
- The delineation of basaltic layers in the upper crust associated with the North Atlantic Igneous Province. These include the Malinstindur, Enni and Beinisdvørð formations, all of which were deposited subaerially.
- The identification of the Lopra Formation, comprised mainly of hyaloclastites, and associated sub-basalt sediments, as a low shear wave velocity layer beneath the overlying basalts, located at depths of approximately 2.5 - 7.0 km.

- The illumination of a high velocity basement layer, which likely corresponds to silicic crystalline rocks of Archaean provenance, and is inferred to have an upper boundary that exhibits significant topography.

The new geological model that we interpret from our results, together with evidence from surface mapping and deep drill holes, indicates that the crust beneath the Faroe Islands is more laterally heterogeneous. This may be a reflection of the processes that lead to the rifting of this continental fragment from the Eurasian margin, although in the case of the basement rocks, it is difficult to ascertain to what extent this heterogeneity is inherited from pre-rift events.

6. Acknowledgements

The Faroe Islands Passive Seismological Experiment (FIPSE) was funded by Sindri (contract C46-52-01) and formed a collaborative project between Dr. David Cornwell, Prof. Richard England (University of Leicester) and Prof. Graham Stuart (University of Leeds). Seismological equipment was loaned from the NERC geophysical equipment facility (GEF, loan 918), with field assistance from David Hawthorn and data processing assistance from Victoria Lane (SEIS-UK). We acknowledge the help, advice and support of Jarðfeingi, especially Thomas Varming, Uni Petersen, Bartal Højgaard, Romica Øster and Heri Ziska. Rannvá M. Arge and Magni Jøkladal are thanked for their assistance with fieldwork. Research undertaken in this article was supported by the Carnegie Trust for the Universities of Scotland, via a Collaborative Research Grant. Rosie Fletcher is thanked for her comments, which greatly improved the text.

References

- Andersen, M. S., 1988. Late Cretaceous and early Tertiary extension and volcanism around the Faeroe Islands. Geological Society, London, Special Publications 39 (1), 115–122.
- Andersen, M. S., Sorensen, A. B., Boldreel, L. O., Nielsen, T., 2002. Cenozoic evolution of the Faroe Platform, comparing denudation and deposition. Geological Society, London, Special Publications 196, 291–311.
- Bais, G., White, R., Worthington, M., Andersen, M., 2008. Seismic properties of Faroe basalts from borehole and surface data , Faroe Islands Exploration Conference: Proceedings of the 2nd Conference. Annales Societatis Scientiarum Færoensis Supplement, 59–75.
- Bensen, G. D., Ritzwoller, M. H., Barmin, M. P., Levshin, A. L., Lin, F., Moschetti, M. P., Shapiro, N. M., Yang, Y., 2007. Processing seismic ambient noise data to obtain reliable broad-band surface wave dispersion measurements. Geophysical Journal International 169 (3), 1239–1260.
- Beyreuther, M., Barsch, R., Krischer, L., Megies, T., Behr, Y., Wassermann, J., 2010. ObsPy: A Python Toolbox for Seismology. Seismological Research Letters 81 (3), 530–533.
- Boldreel, L. O., 2006. Wire-line log-based stratigraphy of flood basalts from the Lopra-1 / 1A well , Faroe Islands. Geological Survey of Denmark and Greenland bulletin 9, 7–22.
- Bott, M. H. P., Sunderland, J., Smith, P. J., Casten, U., Saxov, S., 1974.

- Evidence for continental crust beneath the Faeroe Islands. *Nature* 248, 202–204.
- Brewer, J. a., Smythe, D. K., 1984. MOIST and the continuity of crustal reflector geometry along the Caledonian-Appalachian orogen. *Journal of the Geological Society* 141 (1), 105–120.
- Christensen, N. I., Mooney, W. D., 1995. Seismic velocity structure and composition of the continental crust: A global view. *Journal of Geophysical Research* 100 (B6), 9761.
- Christie, P. A. F., Gollifer, I., Cowper, D., 2006. Borehole seismic studies of a volcanic succession from the Lopra-1/1A borehole in the Faroe Islands, northern North Atlantic. *Geological Survey of Denmark and Greenland Bulletin* 9, 23–40.
- Curtis, a., Gerstoft, P., Sato, H., Snieder, R., Wapenaar, K., 2006. Seismic interferometry – turning noise into signal. *The Leading Edge* 25, 1082–1092.
- Dziewonski, A., Bloch, S., Landisman, M., 1969. A technique for the analysis of transient seismic signals. *Bulletin of the Seismological Society of America* 59 (1), 427–444.
- Eccles, J. D., White, R. S., Robert, A. W., Christie, P. A. F., 2007. Wide angle converted shear wave analysis of a North Atlantic volcanic rifted continental margin : constraint on sub-basalt lithology. *First break* 25 (October), 63–70.

- Ellis, D., Bell, B. R., Jolley, D. W., O'Callaghan, M., 2002. The stratigraphy, environment of eruption and age of the Faroes Lava Group, NE Atlantic Ocean. *Geological Society, London, Special Publications* 197 (1), 253–269.
- England, R. W., McBride, J. H., Hobbs, R. W., 2005. The role of Mesozoic rifting in the opening of the NE Atlantic: evidence from deep seismic profiling across the Faroe. *Journal of the Geological Society* 162 (4), 661–673.
- Hansen, J., Jerram, D. a., McCaffrey, K., Passey, S. R., 2011. Early Cenozoic saucer-shaped sills of the Faroe Islands: an example of intrusive styles in basaltic lava piles. *Journal of the Geological Society* 168 (1), 159–178.
- Heinesen, M. V., Larsen, A., Sorensen, K., 2006. Introduction: Scientific results from the deepened Lopra-1 borehole, Faroe Islands. *Geological Survey of Denmark and Greenland Bulletin* 9, 5–6.
- Herrmann, R. B., 2013. Computer Programs in Seismology : An Evolving Tool for Instruction and Research. *Seismological Research Letters* 84 (6), 1081–1088.
- Kendall, J.-M., Stuart, G. W., Ebinger, C. J., Bastow, I. D., Keir, D., 2005. Magma-assisted rifting in Ethiopia. *Nature* 433 (7022), 146–148.
- Kennett, B. L. N., Sambridge, M. S., Williamson, P. R., 1988. Subspace methods for large scale inverse problems involving multiple parameter classes. *Geophysical Journal* 94, 237–247.
- Lecocq, T., Caudron, C., Brenguier, F., 2014. MSNoise, a Python Package

- for Monitoring Seismic Velocity Changes Using Ambient Seismic Noise. *Seismological Research Letters* 85 (3), 715–726.
- Levshin, A., Pisarenko, V., Pogrebinsky, G., 1972. On a frequency- time analysis of oscillations. *Ann. Geophys* 28 (2), 211–218.
- Luo, Y., Yang, Y., Xu, Y., Xu, H., Zhao, K., Wang, K., 2015. On the limitations of interstation distances in ambient noise tomography. *Geophysical Journal International* 201 (2), 652–661.
- Maresh, J., White, R. S., Hobbs, R. W., Smallwood, J. R., 2006. Seismic attenuation of Atlantic margin basalts: Observations and modeling. *Geophysics* 71 (6), B211–B221.
- Megies, T., Beyreuther, M., Barsch, R., Krischer, L., Wassermann, J., 2011. ObsPy - what can it do for data centers and observatories? *Annals of Geophysics* 54 (1), 47–58.
- Meyer, R., van Wijk, J., Gernigon, L., jan 2007. The North Atlantic Igneous Province: A review of models for its formation. *Geological Society of America Special Papers* 430, 525–552.
- Moy, D., Imber, J., 2009. A critical analysis of the structure and tectonic significance of rift-oblique lineaments ('transfer zones') in the Mesozoic-Cenozoic succession of the Faroe-Shetland Basin, NE Atlantic margin. *Journal of the Geological Society* 166 (5), 831–844.
- Ólavsdóttir J., Eidesgaard, I. R., Stoker, M. S., 2016. The stratigraphy and structure of the Faroese continental margin. In: Pèron-Pinvidic, G; Hopper

- , J.; Stoker, M.S., (eds.) The NE Atlantic Region: a reappraisal of crustal structure, tectonostratigraphy and magmatic evolution. Geological Society of London.
- Osmundsen, P., Sommaruga, A., Skilbrei, J., Olesen, O., 2002. Deep structure of the Mid Norway rifted margin. Norwegian journal of Geology Vol. 82, pp. 205–224.
- Palmason, 1965. Seismic refraction measurements of the lavas of the Faeroe Islands. *Tectonophysics* 2 (6), 475–482.
- Passey, S. R., Bell, B. R., 2007. Morphologies and emplacement mechanisms of the lava flows of the Faroe Islands Basalt Group, Faroe Islands, NE Atlantic Ocean. *Bulletin of Volcanology* 70 (2), 139–156.
- Passey, S. R., Jolley, D. W., 2008. A revised lithostratigraphic nomenclature for the Palaeogene Faroe Islands Basalt Group, NE Atlantic Ocean. Vol. 99. *Earth and Environmental Science Transactions of the Royal Society of Edinburgh*.
- Passey, S. R., Varming, T., 2010. Surface interpolation within a continental flood basalt province: An example from the Palaeogene Faroe Islands Basalt Group. *Journal of Structural Geology* 32 (5), 709–723.
- Petersen, U. K., Brown, R. J., Andersen, M. S., 2013. P-wave velocity distribution in basalt flows of the Enni Formation in the Faroe Islands from refraction seismic analysis. *Geophysical Prospecting* 61 (1), 168–186.
- Petersen, U. K., Brown, R. J., Andersen, M. S., 2015. Geophysical aspects of basalt geology and identification of intrabasaltic horizons *Geophysical*

- aspects of basalt geology and identification of intrabasaltic horizons. In: Faroe Islands Exploration Conference: Proceedings of 4th Conference. *Annales Societatis Scientiarum Færoensis Supplementum LXIV*. No. November. pp. 74–93.
- Petersen, U. K., Funck, T., 2016. Review of velocity models in the Faroe Shetland Channel. In: *The NE Atlantic Region: A Reappraisal of Crustal Structure, Tectonostratigraphy and Magmatic Evolution*. The Geological Society of London, pp. 1–18.
- Rasmussen, J., Noe-Nygaard, A., 1969. *Beskrivelse til geologisk kort over Færøerne i målestok 1:50000*. Geological Survey of Denmark 1.
- Rasmussen, J., Noe-Nygaard, A., 1970. *Geology of the Faeroe Islands*. C. A. Reitzels Forlag.
- Raum, T., Mjelde, R., Berge, A. M., Paulsen, J. T., Digranes, P., Shimamura, H., Shiobara, H., Kodaira, S., Larsen, V. B., Fredsted, R., 2005. Sub-basalt structures east of the Faroe Islands revealed from wide-angle seismic and gravity data. *Petroleum Geoscience* 11 (4), 291–308.
- Rawlinson, N., Sambridge, M., 2004a. Multiple reflection and transmission phases in complex layered media using a multistage fast marching method. *Geophysics* 69 (11), 1338–1350.
- Rawlinson, N., Sambridge, M., 2004b. Wave front evolution in strongly heterogeneous layered media using the fast marching method. *Geophysical Journal International* 156, 631–647.

- Rawlinson, N., Sambridge, M., 2005. The fast marching method: an effective tool for tomographic imaging and tracking multiple phases in complex layered media. *Exploration Geophysics* 36 (4), 341.
- Rawlinson, N., Sambridge, M., Saygin, E., 2008. A dynamic objective function technique for generating multiple solution models in seismic tomography. *Geophysical Journal International* 174 (1), 295–308.
- Richardson, K. R., Smallwood, J. R., White, R. S., Snyder, D. B., Maguire, P. K. H., 1998. Crustal structure beneath the Faroe Islands and the Faroe-Iceland Ridge. *Tectonophysics* 300 (1-4), 159–180.
- Richardson, K. R., White, R. S., England, R. W., Fruehn, J., 1999. Crustal structure east of the Faroe Islands; mapping sub-basalt sediments using wide-angle seismic data. *Petroleum Geoscience* 5, 161–172.
- Ritchie, J. D., Ziska, H., Johnson, H., Evans, D., 2011. Geology of the Faroe-Shetland Basin and adjacent areas. British Geological Survey.
- Rudnick, R. L., Fountain, D. M. 1995. Nature and composition of the continental crust: A lower crustal perspective. *Reviews of Geophysics* 33 (3), 267–309.
- Saunders, A. D., Fitton, J. G., Kerr, A. C., Norry, M. J., Kent, R. W., 1997. The north atlantic igneous province. In: *Large Igneous Provinces: Continental, Oceanic, and Planetary Flood Volcanism*. American Geophysical Union, pp. 45–93.
- Saygin, E., Kennett, B. L. N., 2012. Crustal structure of Australia from

- ambient seismic noise tomography. *Journal of Geophysical Research: Solid Earth* 117 (1).
- Schimmel, M., 1999. Phase cross-correlations: Design, comparisons, and applications. *Bulletin of the Seismological Society of America* 89 (5), 1366–1378.
- Schimmel, M., Gallart, J., 2007. Frequency-dependent phase coherence for noise suppression in seismic array data. *Journal of Geophysical Research: Solid Earth* 112 (4), 1–14.
- Schimmel, M., Paulssen, H., 1997. Noise reduction and detection of weak, coherent signals through phase-weighted stacks. *Geophysical Journal International* 130 (2), 497–505.
- Sethian, J. A., 1996. A fast marching level set method for monotonically advancing fronts. In: *PNAS*. Vol. 93. pp. 1591–1595.
- Smallwood, J. R., Staples, R. K., Richardson, K. R., White, R. S., 1999. Crust generated above the Iceland mantle plume: From continental rift to oceanic spreading center. *Journal of Geophysical Research* 104 (B10), 22,885–22,902.
- Stoker, M., Hitchen, K., Graham, C., 1993. *The Geology of the Hebrides and West Shetland Shelves, and Adjacent Deep-water Areas*. Vol. United Kin. HMSO, London.
- Upton, B. G. J., 1988. History of Tertiary igneous activity in the N Atlantic borderlands. *Geological Society, London, Special Publications* 39 (1), 429–453.

- Waagstein, R., 1988. Structure, composition and age of the Faeroe basalt plateau. Geological Society, London, Special Publications 39 (1), 225–238.
- Waagstein, R., Andersen, C., 2003. Well completion report: Glyvursnes-1 and Vestmanna-1, Faroe Islands. Geological Survey of Denmark and Greenland ISBN 99.
- Waagstein, R., Hald, N., 1984. Structure and petrography of a 660m lava flows from the Vestmanna-1 drill hole, lower and middle basalt series, Faroe Islands. Danmark Geologiske Undersogelse.
- White, R. S., Smallwood, J. R., Fliedner, M. M., Boslaugh, B., Maresh, J., Fruehn, J., 2003. Imaging and regional distribution of basalt flows in the Faeroe-Shetland Basin. Geophysical Prospecting 51 (3), 215–231.

Figure 1: Faroe Islands location and geology. i) Regional topographic and bathymetric map showing the location of the Faroe Islands (red rectangle) in the North Atlantic. ii) Simplified surface geology map and iii) north-south geological cross-section showing the main units of the Faroe Islands Basalt Group (FIBG). ii) and iii) modified from Waagstein (1988). In grey lines are shown the lineaments while in color lines are shown the main refraction studies mentioned in the paper.

Figure 2: Topographic map of the Faroe Islands with surrounding bathymetry. The locations of the twelve seismic stations (IF01–IF12) that comprised the Faroe Islands Passive Seismic Experiment (FIPSE) are shown in yellow.

Figure 3: Record section showing all inter-station cross-correlation functions (CCFs), stacked using phase-weighting (Schimmel et al. 1997, 1999 & 2007) and plotted with respect to inter-station distance.

Figure 4: Two examples of group dispersion results obtained from frequency-time analysis. Normalized amplitude is plotted in color (large amplitudes in red; small amplitudes in blue), and dotted lines represent the dispersion curves used in the inversion for period-dependent group-velocity maps.

Figure 5: Period-dependent group velocity maps at 0.5, 1, 5, 10 and 12 s. B_v = background velocity (in km/s); V_r = variance reduction of data fit (in %). Note that each map is displayed twice, with upper panels showing group velocity with rays superimposed, and lower panels showing % variation in group velocity with respect to the background velocity for each period.

Figure 6: Trade-off curves used to find optimum smoothing and damping parameters for the group velocity maps. Left: Smoothing is held constant (0) while damping is varied between 0 and 1; Right: Damping is held constant (0) while smoothing is varied between 0 and 1. In each case, separate trade-off curves are plotted for periods of 5 s, 10 s and 15 s.

Figure 7: Checkerboard test results for the group velocity maps using three different anomaly sizes: large (diameter 18 km), medium (12.5 km) and small (7 km). Left column shows the input checkerboard, while the output checkerboards for five separate periods are shown in columns 2-6.

Figure 8: Trade-off between mean RMS data misfit and mean model variance for the ensemble of 1-D shear wave velocity models used to build the 3-D shear wave velocity model.

Figure 9: Horizontal slices through the final 3-D shear wave velocity model at 1, 3, 5, 7, 10 and 15 km depth. Note that the same color scale is used for each plot. The checkerboard test results provides insight into which parts of the model are well resolved.

Figure 10: South-north (upper panel, longitude = -6.69°) and west-east (lower panel, latitude = 61.98°) cross-sections through the final S wave 3-D velocity model. The main anomalies are labelled with their respective S wave velocity ranges. Darkened regions denote poorly resolved parts of the velocity model. Grey topography has a maximum elevation of 825 m.

Figure 11: Previous and new interpretation of geological structure beneath the Faroe Islands. a) Integrated interpretation of onshore and offshore seismic refraction surveys (modified from Olavsdottir et al., 2016). b) Interpretation based on the 3-D S wave velocity model shown in Figs. 9 and 10. c) N-S rescaled vertical slice based on the 3-D S wave velocity model shown in Fig. 10. MF = Malinstindur Formation; BF = Beinisdvord Formation; LF = Lopra Formation. Geological layer outlines and borehole locations from a) are superimposed. Grey bar denotes the extent of the Faroe Islands landmass. Vertical exaggeration is approximately 10:1.

H	V _p	V _s	Rho
(km)	(km/s)	(km/s)	(gm/cc)
0.3	3.5	1.5	2
1.0	4.5	2.5	2.4
1.4	5.0	2.7	2.6
3.2	6.0	3.2	2.7
1.1	6.3	3.4	2.8
5.0	6.5	3.7	2.9
5.0	6.9	3.9	3.0
5.0	7.5	4.2	3.1
Moho			
∞	8.25	4.6	3.33

Table 1: Crustal model used for the 1-D shear wave inversion. Values are taken from a variety of sources summarized in Section 1.2.

	V_p (km/s)	V_p/V_s (km/s)	Density (Mg/m ³)
Tertiary basalt	4.4-5.25	1.83-1.85	2.70-2.79
Sub-basalt Mesozoic sediments	4.1-4.3	1.7-1.76	2.50-2.65
Upper basement	5.5-6	1.73	2.7
Crystalline basement	6.1-6.3	1.73-1.77	2.81-2.82
Lower crust	6.75-6.87	1.75-1.81	2.84-2.98
High velocity lower crust	7.25-7.4		3.1-3.12
Upper mantle	8.1-8.25		3.1-3.12

Table 2: Geophysical properties of key layers included in published models (Palmason, 1965; Hall and Simmons, 1979; Richardson et al., 1999; Smallwood et al., 1999; England et al., 2005; Raum et al., 2005; Christie et al., 2006; Eccles et al., 2007; Bais et al., 2008; Petersen et al., 2013).

Borehole	Depth	Formation encountered	P-wave velocity	Vp/Vs
Glyvurnes-1	700 m	-Uppermost 350 m Malinstindur Fm.	4-5 km/s	1.9-2 km/s
		-Lowermost 350 m Enni Fm.	4-6 km/s	1.9-2 km/s
Vestmanna-1	660 m	-Uppermost 60 m Beinivörð Fm.	5-6 km/s	1.8-1.9 km/s
		-Lowermost 600 m Malinstindur Fm.	5-6 km/s	1.8-1.9 km/s
Lopra-1A	3565 m	-Uppermost 2213 m Beinivörð Fm.	4-6 km/s	1.81-1.84 km/s
		-Lowermost 1352 m Lopra Fm.	4-5 km/s	1.81-1.84 km/s

Table 3: Drill depths, P-wave velocity and Vp/Vs for the Glyvurnes-1, Vestmanna-1 and Lopra-1A boreholes (from Waagstein and Andersen, 2003; Petersen et al., 2013, and references therein)

Highlights

- First 3D crustal S-wave velocity model of the Faroe Islands from ambient noise data
- Delineation of basaltic layers of the North Atlantic Igneous Province in the crust
- Identification of the Lopra formation as a sub-basalt low velocity layer
- Strong lateral velocity heterogeneity which may be associated with rifting

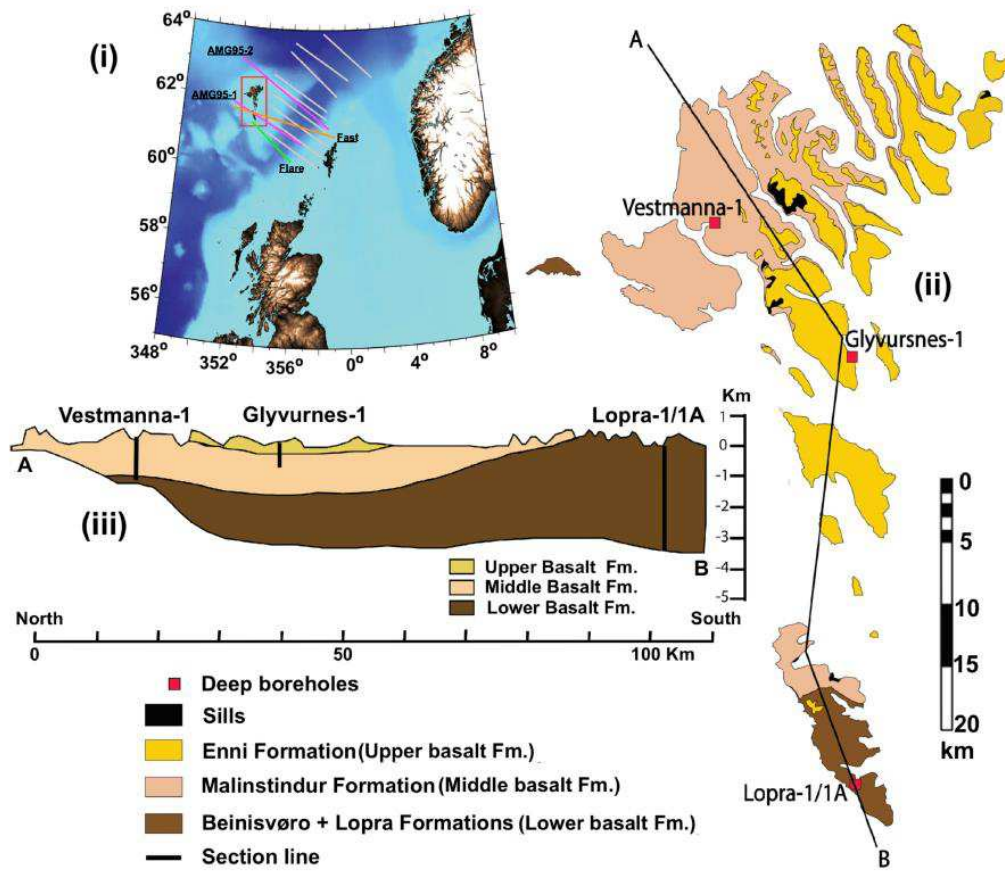


Fig. 1

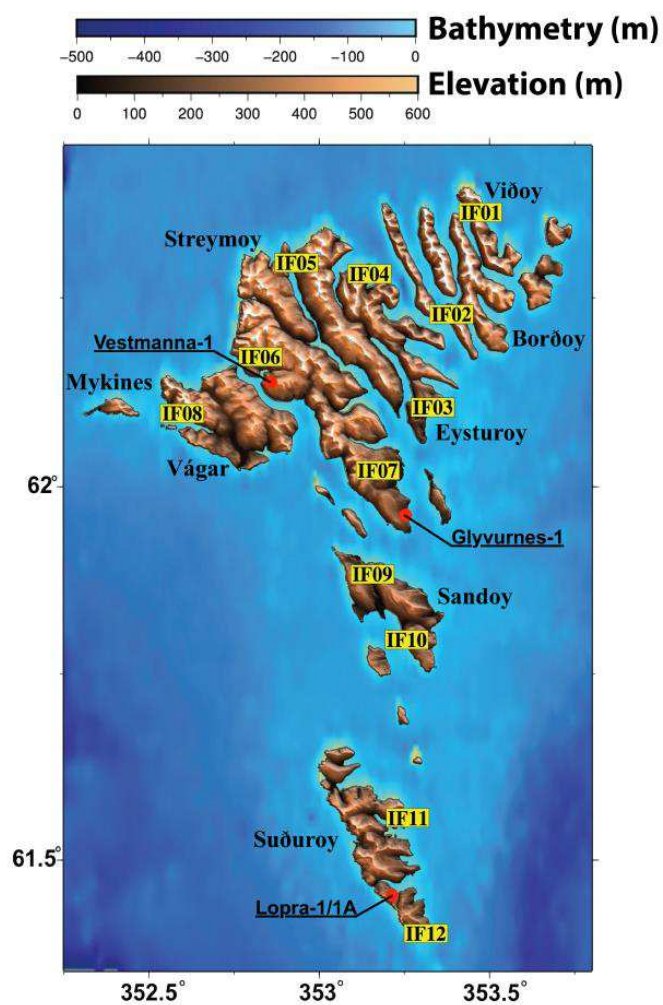


Fig. 2

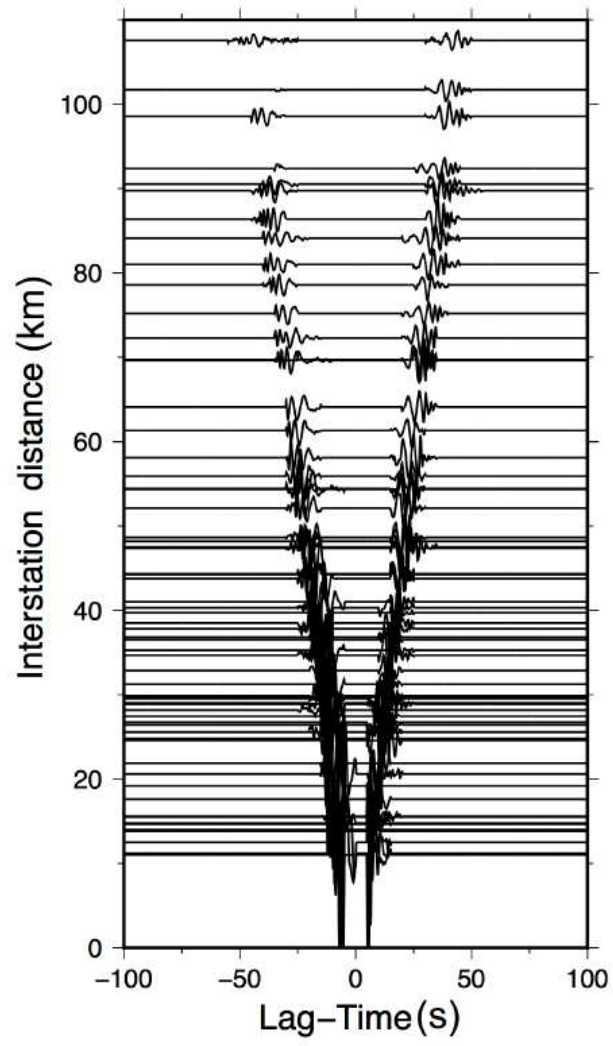


Fig. 3

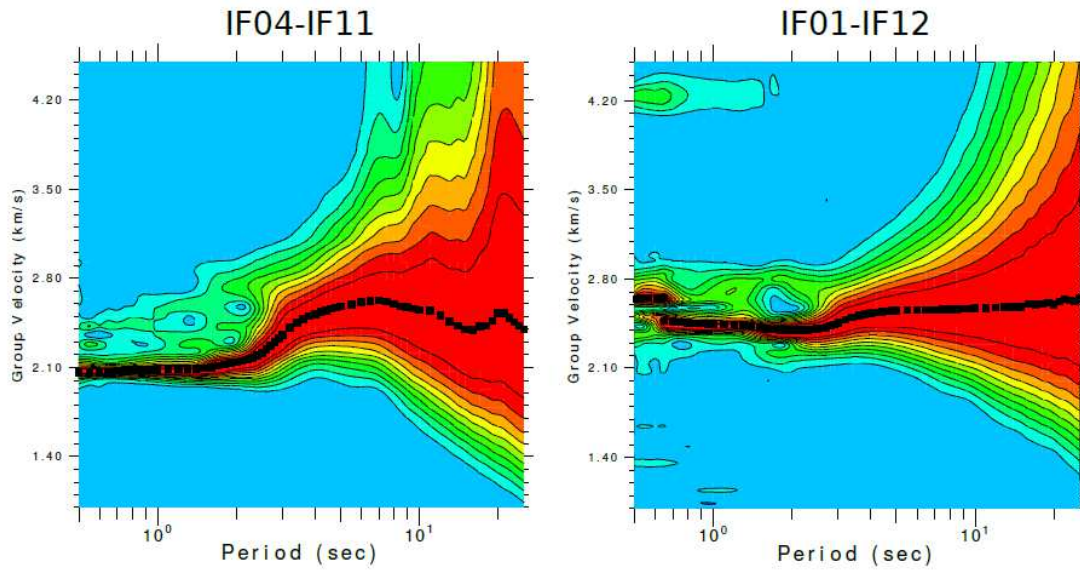


Fig. 4

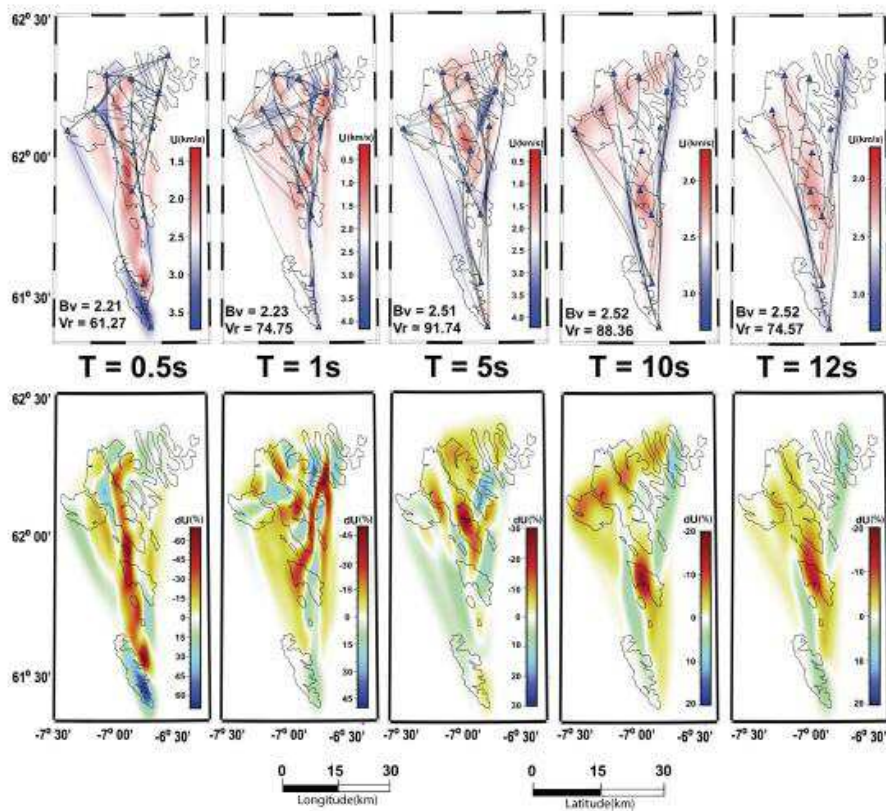


Fig. 5

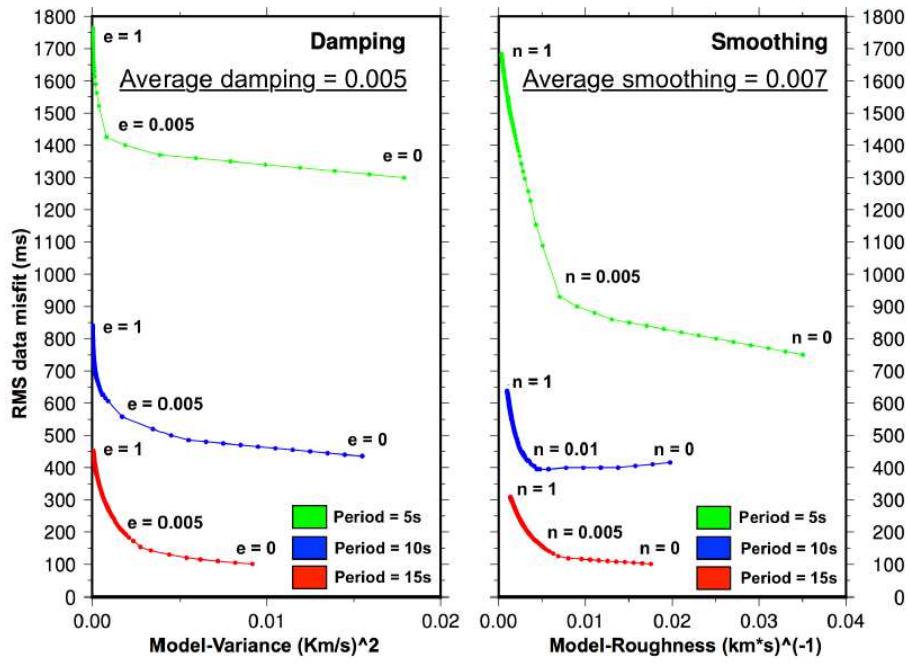


Fig. 6

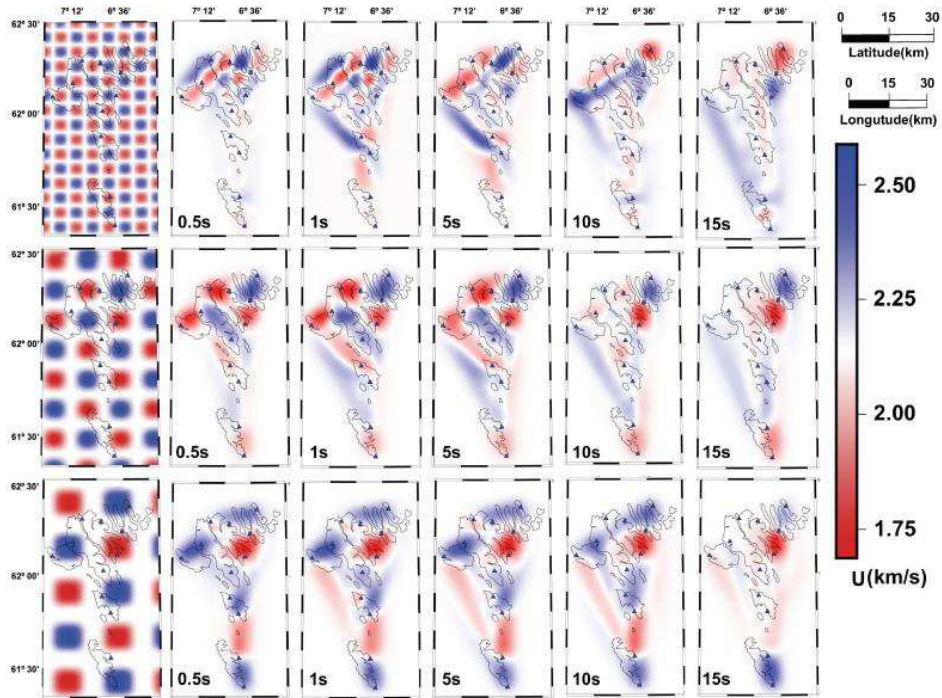


Fig. 7

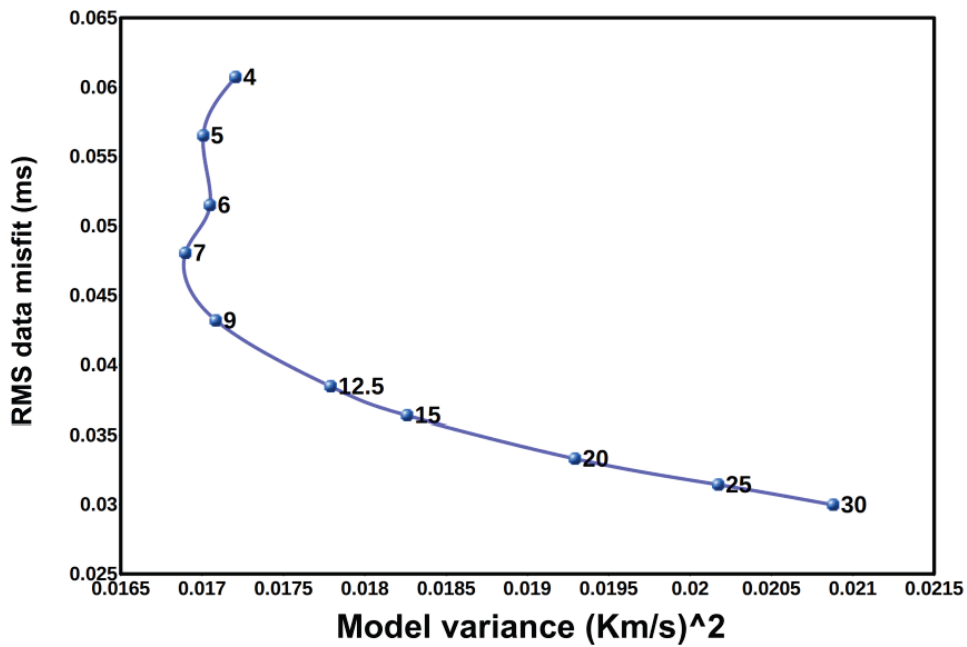


Fig. 8

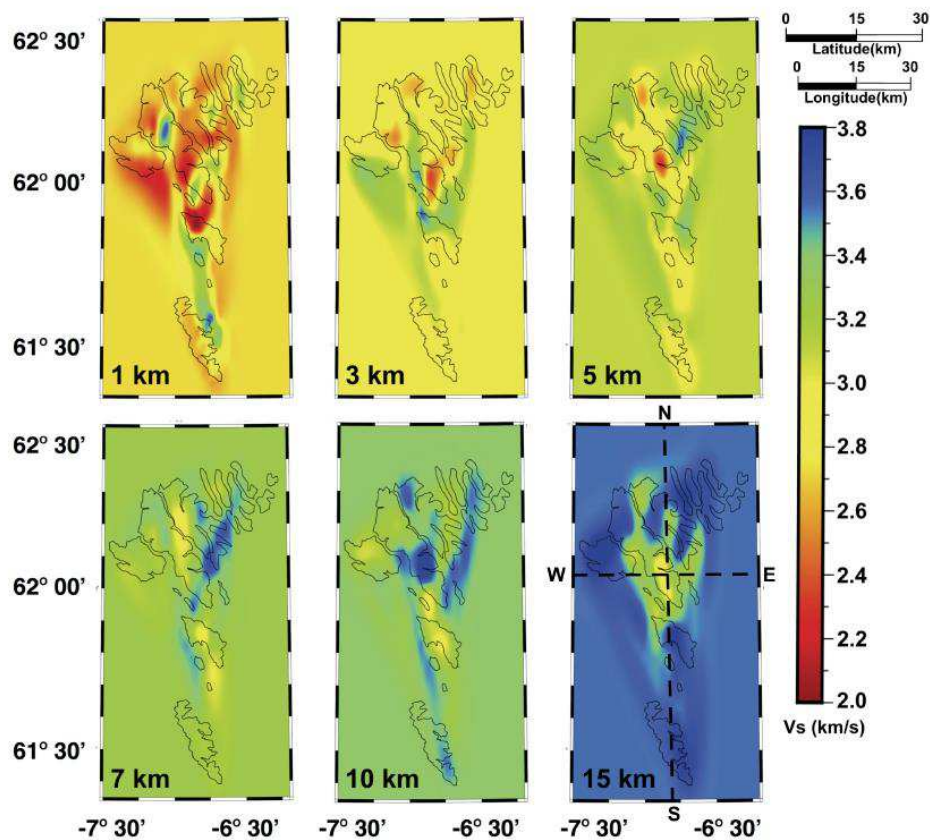


Fig. 9

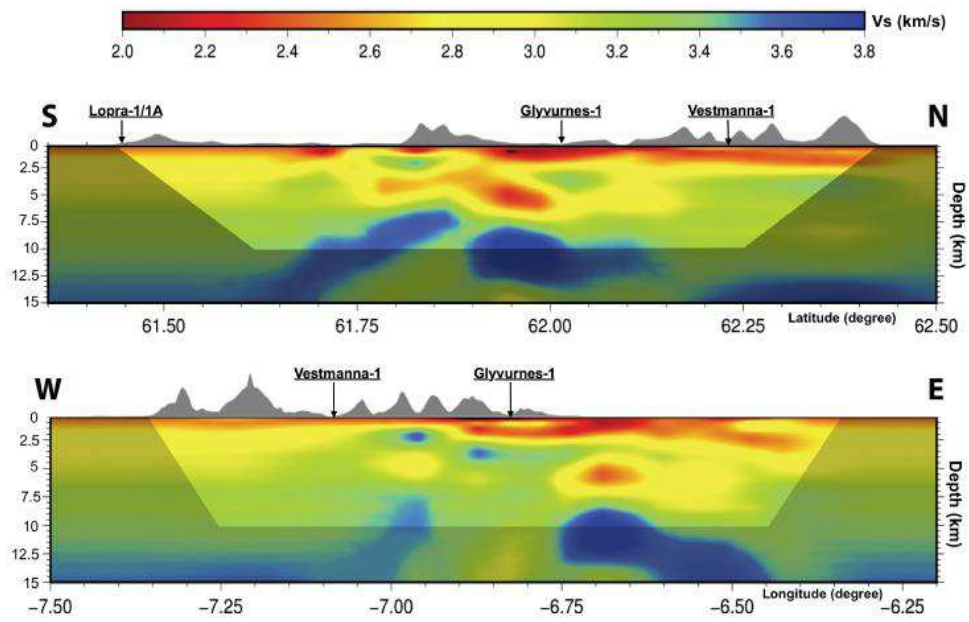


Fig. 10

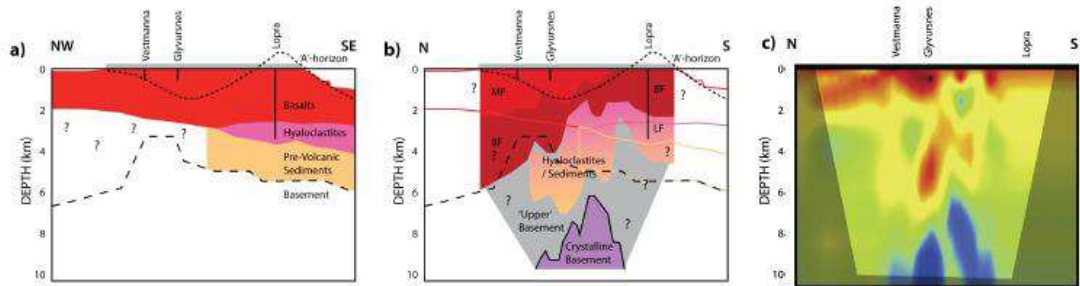


Fig. 11